

Isotopic Constraints on the Atmospheric Sources and Formation of Nitrogenous Species in Biomass-Burning-Influenced Clouds

Yunhua Chang^{1, 2}, Yanlin Zhang^{1*}, Jiarong Li², Chongguo Tian³, Linlin Song⁴,
Xiaoyao Zhai¹, Wenqi Zhang¹, Tong Huang¹, Yu-Chi Lin¹, Chao Zhu², Yunting
5 Fang⁴, Moritz F. Lehmann⁵, and Jianmin Chen^{2*}

¹Yale-NUIST Center on Atmospheric Environment, Nanjing University of Information Science & Technology, Nanjing 210044, China.

²Shanghai Key Laboratory of Atmospheric Particle Pollution and Prevention (LAP³), Department of Environmental Science & Engineering, Institute of Atmospheric Sciences, Fudan University,
10 Shanghai 200433, China.

³Key Laboratory of Coastal Environmental Processes and Ecological Remediation, Yantai Institute of Coastal Zone Research, Chinese Academy of Sciences, Yantai 264003, China.

⁴CAS Key Laboratory of Forest Ecology and Management, Institute of Applied Ecology, Chinese Academy of Sciences, Shenyang 110016, China.

15 ⁵Aquatic and Isotope Biogeochemistry, Department of Environmental Sciences, University of Basel, Basel 4056, Switzerland.

*Corresponding authors: Yanlin Zhang (dryanlinzhang@outlook.com) and Jianmin Chen (jmchen@fudan.edu.cn).

Abstract

Predicting tropospheric cloud formation and subsequent nutrient deposition relies on 25 understanding the sources and processes affecting aerosol constituents of the atmosphere that are preserved in cloudwater. However, this challenge is difficult to address quantitatively based on the sole use of bulk chemical properties. Nitrogenous aerosols, mainly ammonium (NH_4^+) and nitrate (NO_3^-), play a particularly important role in tropospheric cloud formation. While dry and wet (mainly rainfall) deposition of NH_4^+ and NO_3^- are regularly assessed, cloudwater deposition is 30 often underappreciated. Here we collected cloudwater samples at the summit of Mt. Tai (1545 m above sea level) in Eastern China during a long-lasting biomass burning (BB) event, and simultaneously measured for the first time the isotopic compositions (mean $\pm 1\sigma$) of cloudwater nitrogen species ($\delta^{15}\text{N}-\text{NH}_4^+ = -6.53 \pm 4.96\text{\textperthousand}$, $\delta^{15}\text{N}-\text{NO}_3^- = -2.35 \pm 2.00\text{\textperthousand}$, $\delta^{18}\text{O}-\text{NO}_3^- = 57.80 \pm 4.23\text{\textperthousand}$), allowing insights into their sources and potential transformation mechanism within the 35 clouds. Large contributions of BB to the cloudwater NH_4^+ ($32.9 \pm 4.6\%$) and NO_3^- ($28.2 \pm 2.7\%$) inventories were confirmed through a Bayesian isotopic mixing model, coupled with our newly-developed computational quantum chemistry module. Despite an overall reduction in total 40 anthropogenic NO_x emission due to effective emission control actions and stricter emission standards for vehicles, the observed cloud $\delta^{15}\text{N}-\text{NO}_3^-$ values suggest that NO_x emissions from transportation may have exceeded emissions from coal combustion. $\delta^{18}\text{O}-\text{NO}_3^-$ values imply that 45 the reaction of OH with NO_2 is the dominant pathway of NO_3^- formation ($57 \pm 11\%$), yet the contribution of heterogeneous hydrolysis of dinitrogen pentoxide was almost as important ($43 \pm 11\%$). Although the limited sample set used here results in a relatively large uncertainty with regards to the origin of cloud-associated nitrogen deposition, the high concentrations of inorganic nitrogen imply that clouds represent an important source of nitrogen, especially for nitrogen-

limited ecosystems in remote areas. Further simultaneous and long-term sampling of aerosol, rainfall, and cloudwater is vital for understanding the anthropogenic influence on nitrogen deposition in the study region.

1 Introduction

50 Nitrogenous aerosols, mainly nitrate (NO_3^-) and ammonium (NH_4^+), formed from the emissions of nitrogen oxides ($\text{NO}_x = \text{NO} + \text{NO}_2$) and ammonia (NH_3), are major chemical components of aerosols, which serve as cloud condensation nuclei (CCN) and thus play an important role during cloud formation in the troposphere (Gioda et al., 2011; van Pinxteren et al., 2016). Cloudwater-containing nitrogenous compounds also represent a vital contributor to 55 nitrogen (N) budgets of terrestrial (Li et al., 2016b; Liu et al., 2013; Weathers and Likens, 1997; Vega et al., 2019) and marine ecosystems (Kim et al., 2014; Okin et al., 2011). However, the sources and formation processes of cloudwater N species are only poorly understood.

NO_x can be emitted from both anthropogenic and natural sources. Globally, over 50% of 60 the NO_x emissions derive from combustion of fossil fuel ($\sim 25 \text{ Tg N yr}^{-1}$; Jaegle et al., 2005; Richter et al., 2005; Duncan et al., 2016), with the remainder being primarily soil-related emissions ($\sim 9 \text{ Tg N yr}^{-1}$; Lamsal et al., 2011; Price et al., 1997; Yienger et al., 1995; Miyazaki et al., 2017), or deriving from biomass burning ($\sim 6 \text{ Tg N yr}^{-1}$), and lightning ($2\text{-}6 \text{ Tg N yr}^{-1}$) (Anenberg et al., 2017; Levy et al., 1996). The atmospheric sinks of NO_x include the production of HNO_{3(g)} and the 65 formation of aerosol NO_{3⁻} (Seinfeld and Pandis, 2012), the partitioning of which can vary with time (Morino et al., 2006). As for NH₃, over 90% of the NH₃ emissions in terrestrial ecosystems originate from agricultural production, such as livestock breeding and NH₃-based fertilizer application (Poulton et al., 2014; Kang et al., 2016; Reis et al., 2009; Bouwman et al., 1997; Heald et al., 2012; Zhang et al., 2018; Balasubramanian et al., 2015; Huang et al., 2011). In the urban

atmosphere, recent studies suggest that non-agricultural activities like wastewater discharge
70 (Zhang et al., 2017), coal burning (Li et al., 2016a), solid waste (Reche et al., 2012), on-road traffic
(Suarez-Bertoa et al., 2014), and green space (Teng et al., 2017) also contribute to NH_3 emissions. In reactions with H_2SO_4 and HNO_3 , NH_3 contributes to the formation of NH_4^+ salts, which typically make up from 20 to 80% of fine particle ($\text{PM}_{2.5}$) in the atmosphere (Seinfeld and Pandis, 2012).

75 Biomass burning (BB) is an important source of N in the atmosphere (Lobert et al., 1990; Souri et al., 2017). During the harvest/hot season of eastern China, agricultural BB frequently occurs and modifies the concentration and composition of aerosols in the atmosphere (Chen et al., 2017; Zhang and Cao, 2015). For example, about 50% of the N derived from biomass combustion can be released as NH_3 and NO_x to form particulate NH_4^+ and NO_3^- , which then account for over 80 80% of total nitrogenous species in BB smoke particles (Crutzen and Andreae, 1990). BB-induced aerosols have not only been associated with poor air quality and the detrimental effects on human health, they have also shown to exert manifold effects on tropospheric clouds, altering regional or even global radiation budgets (Chen et al., 2014; Norris et al., 2016; Voigt and Shaw, 2015).

85 The optical and chemical properties of clouds (and thus their radiative forcing) are directly related to the aerosol and precipitation chemistry (Seinfeld et al., 2016). Moreover, clouds represent reactors of multiphase chemistry, contributing to many chemical transformations that would otherwise not take place, or would proceed at much slower rates (Herrmann et al., 2015; Lance et al., 2017; Ravishankara, 1997; Schurman et al., 2018; Slade et al., 2017). Understanding 90 the sources and fate of nitrogenous species in BB-influenced clouds is particularly important to comprehensively assess the environmental impacts of BB. But this challenge is difficult to address based on the sole use of bulk chemical properties (as most often done in previous studies).

Given that the ^{15}N can be preserved between the sources and sinks of NO_x and NH_3 , the N isotopic composition of NO_3^- ($\delta^{15}\text{N-NO}_3^-$) and NH_4^+ ($\delta^{15}\text{N-NH}_4^+$) can be related to different sources of NO_x and NH_3 , and thus delivers useful information regarding the partitioning of the 95 origins of atmospheric/cloudwater NO_x and NH_3 , respectively (Hastings et al., 2013; Michalski et al., 2005; Morin et al., 2008; Chang et al., 2018). This is different for the O isotopes. NO_3^- production involves the oxidation of NO . The first step in the overall process is the conversion of NO into NO_2 , e.g., through the oxidation by either ozone (O_3) or peroxy radicals (Michalski et al., 2011). Significant ^{18}O enrichments and excess ^{17}O (i.e., clear evidence for mass independent 100 fractionation) are observed in atmospheric NO_3^- collected across the globe (e.g., Michalski et al., 2005; Hastings et al., 2003). Such diagnostic isotope signatures, as well as their variability in space and time have been linked to the extent of O_3 oxidation (Michalski et al., 2011). Put another way, the oxygen isotope composition of NO_3^- ($\delta^{18}\text{O-NO}_3^-$) is largely determined by chemical reactions rather than the source, and it is primarily modulated by the O-atom exchange (Michalski et al., 105 2011). in the atmosphere Therefore, $\delta^{18}\text{O-NO}_3^-$ has the potential to indicate the relative importance of various NO_3^- formation pathways (i.e., oxidation pathways during conversion of nitrogen oxides to NO_3^-) (Alexander et al., 2009; Elliott et al., 2009).

The O isotope fractionation during the conversion of NO_x to $\text{HNO}_3/\text{NO}_3^-$

($\frac{\varepsilon_{\text{O}(\text{NO}_x \leftrightarrow \text{HNO}_3)} / \varepsilon_{\text{O}(\text{NO}_x \leftrightarrow \text{NO}_3^-)}$) involves two oxidation pathways (Hastings et al., 2003)

$$\begin{aligned}
 \varepsilon_{\text{O}(\text{NO}_x \leftrightarrow \text{NO}_3^-)} &= \varepsilon_{\text{O}(\text{NO}_x \leftrightarrow \text{HNO}_3)} = \gamma \times \varepsilon_{\text{O}(\text{NO}_x \leftrightarrow \text{NO}_3^-)_{\text{OH}}} + (1 - \gamma) \times \varepsilon_{\text{O}(\text{NO}_x \leftrightarrow p\text{NO}_3^-)_{\text{H}_2\text{O}}} \\
 &= \gamma \times \varepsilon_{\text{O}(\text{NO}_x \leftrightarrow \text{HNO}_3)_{\text{OH}}} + (1 - \gamma) \times \varepsilon_{\text{O}(\text{NO}_x \leftrightarrow \text{HNO}_3)_{\text{H}_2\text{O}}}
 \end{aligned} \tag{1}$$

where $\gamma/(1-\gamma)$ represents the contribution ratio of the isotope fractionation associated with

the formation of $\text{HNO}_3/\text{NO}_3^-$ through the “ $\text{OH}+\text{NO}_2$ ” pathway ($\varepsilon_{\text{O}(\text{NO}_x \leftrightarrow \text{NO}_3^-)_{\text{OH}}}$) and the hydrolysis

of dinitrogen pentoxide (N_2O_5) ($\varepsilon_{\text{O}(\text{NO}_x \leftrightarrow \text{NO}_3^-)_{\text{H}_2\text{O}}}$), respectively. The $\delta^{18}\text{O}$ value of HNO_3 produced by the former process reflects the O atom partitioning of $2/3 \text{ O}_3$ and $1/3 \text{ OH}$:

$$\begin{aligned} \varepsilon_{\text{O}(\text{NO}_x \leftrightarrow \text{NO}_3^-)_{\text{OH}}} &= \varepsilon_{\text{O}(\text{NO}_x \leftrightarrow \text{HNO}_3)_{\text{OH}}} = \frac{2}{3} \varepsilon_{\text{O}(\text{NO}_2 \leftrightarrow \text{HNO}_3)_{\text{OH}}} + \frac{1}{3} \varepsilon_{\text{O}(\text{NO} \leftrightarrow \text{HNO}_3)_{\text{OH}}} \\ &= \frac{2}{3} \left[\frac{1000 \left(\frac{18}{\text{NO}_2/\text{NO}} - 1 \right) \left(1 - f_{\text{NO}_2} \right)}{\left(1 - f_{\text{NO}_2} \right) + \left(\frac{18}{\text{NO}_2/\text{NO}} \times f_{\text{NO}_2} \right)} + \left(\delta^{18}\text{O-NO}_x \right) \right] + \\ &\quad \frac{1}{3} \left[\left(\delta^{18}\text{O-H}_2\text{O} \right) + 1000 \left(\frac{18}{\text{OH/H}_2\text{O}} - 1 \right) \right] \end{aligned} \quad (2)$$

115

As for the $\delta^{18}\text{O}$ value of HNO_3 formed during hydrolysis of N_2O_5 , $5/6$ of the O atoms is derived from O_3 and $1/6$ from OH (Hastings et al., 2003):

$$\varepsilon_{\text{O}(\text{NO}_x \leftrightarrow \text{NO}_3^-)_{\text{H}_2\text{O}}} = \varepsilon_{\text{O}(\text{NO}_x \leftrightarrow \text{HNO}_3)_{\text{H}_2\text{O}}} = \frac{5}{6} \left(\delta^{18}\text{O-N}_2\text{O}_5 \right) + \frac{1}{6} \left(\delta^{18}\text{O-H}_2\text{O} \right) \quad (3)$$

where f_{NO_2} refers to the fraction of NO_2 in the total NO_x pool. Values for f_{NO_2} vary

120 between 0.2 and 0.95 (Walters and Michalski, 2015). $\delta^{18}\text{O-X}$ is the O isotopic composition of X.

The range of $\delta^{18}\text{O-H}_2\text{O}$ can be approximated using an estimated tropospheric water vapor $\delta^{18}\text{O}$ range of $-25\text{‰}-0\text{‰}$ (Zong et al., 2017). The $\delta^{18}\text{O}$ of NO_2 and N_2O_5 varies between 90‰ and 122‰

(Zong et al., 2017). $\frac{18}{\text{NO}_2/\text{NO}}$ and $\frac{18}{\text{OH/H}_2\text{O}}$ represent the equilibrium O isotope fractionation factor between NO_2 and NO , and OH and H_2O , respectively, which is temperature-dependent

$$1000 \left(\frac{m}{\text{NO}_2/\text{NO}} - 1 \right) = \frac{A}{T^4} \times 10^{10} + \frac{B}{T^3} \times 10^8 + \frac{C}{T^2} \times 10^6 + \frac{D}{T} \times 10^4 \quad (4)$$

125

where A, B, C, and D are experimental constants over the temperature range of 150-450 K. Based on Equations 1-4 and measured values for $\delta^{18}\text{O-NO}_3^-$ of cloudwater, a Monte Carlo simulation was performed to generate 10000 feasible solutions. The error between predicted and measured $\delta^{18}\text{O}$ was less than 0.5‰.

130 End of July 2015, a large-scale BB event occurred over eastern and northern China. We took advantage of this special event to collect cloudwater samples at a high-altitude mountaintop site in the North China Plain, and to calibrate the isotopic signatures that BB events leave in the N pool of clouds. Integrating cloudwater nitrogenous species isotope data ($\delta^{15}\text{N-NH}_4^+$, $\delta^{15}\text{N-NO}_3^-$ and $\delta^{18}\text{O-NO}_3^-$) in a Bayesian isotopic mixing model coupled with a newly developed 135 computational quantum chemistry module (Chang et al., 2018), and using an isotopic mass balance approach, the sources and production pathways of inorganic nitrogen in cloudwater were quantified. Although numerous studies have been conducted that involved the chemical characterization of fog water or cloudwater, to our knowledge, there are no reports on the N (and O) isotopic composition of both NO_3^- and NH_4^+ in cloudwater.

140 **2 Materials and Methods**

2.1 Cloudwater Sample Collection

Mt. Tai (117°13' E, 36°18' N; 1545 m above sea level) is a world-recognized geopark of key natural, historical and cultural significance, located in the eastern North China Plain (Fig. 1). It belongs to China's most important agricultural and industrial production areas, and the 145 composition of the atmosphere near the mountain can be considered representative with regards to the quality and levels of atmospheric pollution in the region (Li et al., 2017; Liu et al., 2018). Given the opportunistic nature of this study, cloudwater sampling commenced at the summit of

Mt. Tai three days after the fire began (08/01/2015 19:12 to 08/03/2015 6:12; Table 1). In total, six cloudwater samples were collected during the long-lasting cloud event using a single-stage

150 Caltech active strand cloud-water collector (CASCC), as described by (Demoz et al., 1996). The cloud collector was cleaned prior to each sampling using high-purity deionized water. After sampling, cloud samples were filtered immediately using disposable syringe filters (0.45 μm) to remove any suspended particulate matter, and then stored in a freezer at -80 $^{\circ}\text{C}$ until further analysis. More details on the monitoring site and sampling procedures can be found elsewhere (Li

155 et al., 2017).

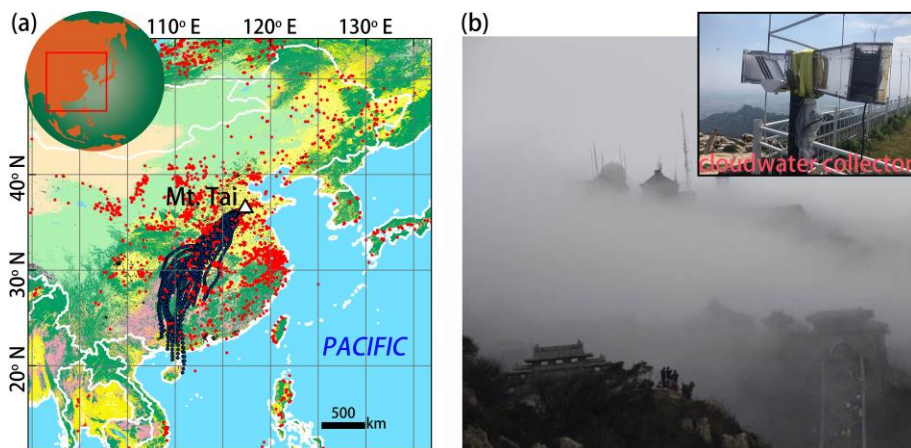


Figure 1. (a) Location of Mt. Tai (triangle) and twenty-four 48-h back trajectories (black lines) of air masses simulated by the HYSPLIT model (<http://ready.arl.noaa.gov/HYSPLIT.php>) based on the Global Data Assimilation System (GDAS) meteorological data set arriving at Mt. Tai 160 on 1 August 2015 (4:00 UTC) at an altitude 1500-m a.s.l (close to the altitude of our sampling site). The base map of land use in China was modified from Chang et al. (2018). The red dots represent the positions of wildfires between 29 and 31 July 2015, based on moderate-resolution imaging spectroradiometer (MODIS) (<http://modis-fire.umd.edu>). (b) Field photos of clouds-shrouded Mt. Tai and the cloudwater collector.

165 **2.2 Chemical and Isotopic Analysis**

Inorganic ions (including SO_4^{2-} , NO_3^- , Cl^- , NH_4^+ , K^+ , Ca^{2+} , Mg^{2+} , and Na^+), as well as levoglucosan, a specific tracer of biomass burning, in cloudwater samples were analyzed using a DionexTM ICS-5000⁺ system (ThermoFisher Scientific, Sunnyvale, USA). The IC system was equipped with an automated sampler (AS-DV). Cloudwater samples were measured using an 170 IonPac CG12A guard column and a CS12A separation column, with an aqueous methanesulfonic acid (MSA, 30 mM L⁻¹) eluent at a flow rate of 1 mL min⁻¹. Detailed information regarding sample processing, pre-treatment, chemical analyses, and analytical protocol adaption can be found elsewhere (Cao et al., 2016, 2017). The detection limits for Na^+ , NH_4^+ , K^+ , Mg^{2+} , Ca^{2+} , Cl^- , NO_2^- , 175 NO_3^- , SO_4^{2-} , and levoglucosan are 0.06, 0.03, 0.12, 0.08, 0.13, 0.64, 1.11, 2.67, 1.41, and 1.29 ppb, respectively. The analytical errors from duplicate analysis were within 5%.

Analysis of the isotopic compositions of NH_4^+ ($\delta^{15}\text{N-NH}_4^+$) and NO_3^- , ($\delta^{15}\text{N-NO}_3^-$ and $\delta^{18}\text{O-NO}_3^-$) was based on the isotopic analysis of nitrous oxides (N_2O) after chemical conversion of the respective target compound. More precisely, dissolved NH_4^+ in cloudwater samples was oxidized to NO_2^- by alkaline hypobromite (BrO^-), and then reduced to N_2O by hydroxylamine 180 hydrochloride ($\text{NH}_2\text{OH.HCl}$) (Liu et al., 2014). NO_3^- was initially transformed to NO_2^- by cadmium, and then further reduced to N_2O by sodium azide (NaN_3) in an acetic acid buffer (McIlvin and Altabet, 2005; Tu et al., 2016). The produced N_2O was analyzed using a purge and cryogenic trap system (Gilson GX-271, IsoPrime Ltd., Cheadle Hulme, UK), coupled to an isotope ratio mass spectrometer (PT-IRMS) (IsoPrime 100, IsoPrime Ltd., Cheadle Hulme, UK). In order 185 to correct for any machine drift and procedural blank contribution, international NH_4^+ (IAEA N1, USGS 25, and USGS 26) and NO_3^- (IAEA N3, USGS 32, and USGS 34) standards were processed in the same way as samples. Standard regressions were made based on the known isotopic values

of international standards and the measured standard $\delta^{15}\text{N}$ values. The slope of the plot of the sample versus the standard $\delta^{15}\text{N}$ (0.49) was very close to the expected slope (0.5), which can be predicted based on the fact that half of the N atoms were derived from the azide (McIlvin and Altabet, 2005). The r^2 of the regression line was 0.999. The analytical precision for both multiple N and O isotopic analyses was better than 0.3‰ ($n = 5$).

2.3 Bayesian Mixing Model Analysis

By taking the uncertainty associated with the N isotopic signatures of multiple sources and associated isotope fractionation during (trans-)formations into account, the Bayesian method is more appropriate than simple linear mixing modeling to yield estimates on the source partitioning of a mixture like air pollutants (Chang et al., 2016; Chang et al., 2018). The relative contribution of each source in Bayesian theorem is expressed as:

$$P(f_q | data) = \theta(data | f_q) \times P(f_q) / \sum \theta(data | f_q) \times P(f_q)$$

where $\theta(\text{data}|f_q)$ and $P(f_q)$ represent the likelihood of the given mixed isotope signature, and the pre-determined probability of the given state of nature, based on prior information, respectively. The denominator represents the numerical approximation of the marginal probability of the data. Here the Bayesian mixing model MixSIR (stable isotope mixing models using sampling-importance-resampling) was used to disentangle the various potential NH_3 and NO_x sources contributing to the cloudwater NH_4^+ and NO_3^- pools, respectively, by forming the true probability distributions through generating 10000 solutions of source apportionment. Details on the model approach can be found in SI Text S1.

The measured $\delta^{15}\text{N-NO}_3^-$ values of cloudwater samples depend on the $\delta^{15}\text{N}$ signatures of the original NO_x sources ($\delta^{15}\text{N-NO}_x$), the N isotope fractionation between nitrogen oxides (i.e.,

210 NO and NO₂ (Walters et al., 2016)), and the N isotope enrichment factor (ε_N) associated with the kinetic transformation of NO_x to HNO₃ (Walters and Michalski, 2015). ε_N is considered a hybrid of two dominant processes: one is the reaction of NO₂ and OH radicals to form NO₃⁻, the other is the heterogeneous hydrolysis of dinitrogen pentoxide (N₂O₅) with water to form NO₃⁻. We recently developed a quantum chemistry computation module to quantify the N fractionation during nitrate formation, which had been validated by field measurements (Chang et al., 2018). Here this module was adopted to calculate the N isotope fractionation during NO₃⁻ formation, and in turn to correct the raw $\delta^{15}\text{N}$ -NO₃⁻ values of cloudwater samples.

215 While the N isotopic source signatures of NO_x are relatively well constrained (Table S1), this is not the case for NH₃. We recently established a pool of isotopic source signatures of NH₃ in 220 eastern China, in which livestock breeding and fertilizer application were identified to produce NH₃ with a $\delta^{15}\text{N}$ of $-29.1 \pm 1.7\text{\textperthousand}$ and $-50.0 \pm 1.8\text{\textperthousand}$, respectively (Chang et al., 2016). Although fossil-fuel combustion, urban waste, and natural soils also represent potential sources of NH₃, their 225 impacts are probably minor compared to that of agricultural and biomass burning emissions, at least on a regional (or greater) scale (Kang et al., 2016). For the N isotope signature of biomass burning-derived NH₃ we assumed 12‰ (Kawashima and Kurahashi, 2011), a value that has also been applied in other recent isotope-based source apportionment studies (e.g., Chellman et al., 2016; Wang et al., 2017a).

3 Results and Discussion

3.1 Chemical characterization of biomass-burning-influenced clouds

230 The moderate-resolution imaging spectroradiometer (MODIS) wildfire map (Fig. 1) shows that there were intensive biomass burning events occurring over mainland China, end of July 2015,

just before the study period. Moreover, analysis of the back trajectories of air masses at the study site revealed the strong influence by atmospheric transport from regions that also experienced intensive biomass burning events shortly before the sampling campaign. It can thus be assumed
235 that large amounts of BB-related pollutants were transported from the southwest to the sampling site at Mt. Tai. Table 1 compiles sample information and results from the chemical and isotopic analysis of cloudwater samples in this study. The concentrations of NO_3^- and NH_4^+ ranged from 4.9 to 19.9 mg L^{-1} (10.1 mg L^{-1} on average), and from 4.9 to 18.0 mg L^{-1} (9.1 mg L^{-1} on average), respectively, much higher than during non-BB seasons (Chen et al., 2017; Desyaterik et al., 2013;
240 Li et al., 2017, 2018; Lin et al., 2017). Similarly, levoglucosan in our cloudwater samples varied between 12.1 and 35.1 $\mu\text{g L}^{-1}$ (19.9 $\mu\text{g L}^{-1}$ on average), and concentrations were thus one order of magnitude higher than those documented during non-BB seasons (Boone et al., 2015; Fomba et al., 2015). Although levoglucosan can be oxidized by OH radicals in the tropospheric aqueous phase (Sang et al., 2016), it is nevertheless a reliable marker compound for BB due to its high
245 emission factors and relatively high concentrations in the ambient aerosols (Hoffmann et al., 2010). In our study, the concentrations of NO_3^- ($r^2 = 0.55$) and NH_4^+ ($r^2 = 0.66$) are strongly correlated with that of levoglucosan, suggesting that the pronounced increase of NO_3^- and NH_4^+ levels observed here can at least be partly attributed to BB activities during the study period. Globally, BB accounts for around 10% of NH_3 and NO_x emissions (Benkovitz et al., 1996; Bouwman et al.,
250 1997; Olivier et al., 1998; Schlesinger and Hartley, 1992).

Table 1. Sampling details and results of chemical and isotopic analysis for collected

255 cloudwater samples.

Date	Local time	NO_3^- (mg L ⁻¹)	NH_4^+ (mg L ⁻¹)	levoglucosan ($\mu\text{g L}^{-1}$)	$\delta^{15}\text{N-NO}_3^-$ (‰)	$\delta^{18}\text{O-NO}_3^-$ (‰)	$\delta^{15}\text{N-NH}_4^+$ (‰)
Aug 1	19:12-22:58	19.86	17.99	35.06	-0.22	65.46	3.62
	23:45-08:25	4.88	4.92	12.11	-1.28	55.01	3.85
Aug 2	09:10-12:19	5.57	5.81	23.60	-0.40	59.84	0.05
	12:55-18:30	13.24	11.51	18.67	-4.18	55.66	11.34
	20:02-23:06	10.06	7.74	13.63	-3.11	56.63	12.99
	23:48-06:12	6.71	6.59	16.42	-4.92	54.19	7.33

3.2 Isotopic characterization of biomass-burning-influenced clouds

The N (and O) isotopic composition of cloudwater nitrogenous species was more (NH_4^+) or less (NO_3^-) variant (Table 1), with the average $\delta^{15}\text{N}$ values of 6.53‰ and -2.35‰ for NH_4^+ and NO_3^- , respectively. The average $\delta^{18}\text{O-NO}_3^-$ value was 57.80‰. These values are generally different from gas, rainwater, and aerosol values measured worldwide (Fig. 2). Various atmospheric processes can influence the isotopic composition of atmospheric nitrogenous species including: the original emission source of NO_x , seasonality of oxidation pathways, isotope fractionation during transport, partitioning between wet and dry components, and spatial gradients in atmospheric chemistry (Elliott et al., 2007; Hastings et al., 2003). These aspects may affect the $\delta^{15}\text{N}$ and $\delta^{18}\text{O}$ values differentially. For example, the $\delta^{15}\text{N}$ of atmospheric NO_3^- retains spatial changes in the original NO_x signature quite well, in contrast to the $\delta^{18}\text{O}$. On the other hand, the $\delta^{18}\text{O}$ most strongly depends on the oxidation chemistry and formation pathway in the atmosphere (see Equations 1-4).

270 At present, there are no other reports on the isotope ratios of both NO_3^- and NH_4^+ in
cloudwater, and a comparison is possible only with isotope data from precipitation and aerosol N.
Recently, Vega et al. (2019) reported the $\delta^{15}\text{N}$ ($-8\text{\textperthousand} \pm 2\text{\textperthousand}$) and $\delta^{18}\text{O}$ ($71\text{\textperthousand} \pm 3\text{\textperthousand}$) values of NO_3^-
in fog water at a forest site in Sweden. The relatively high $\delta^{15}\text{N}$ values in our study ($-2.35\text{\textperthousand}$)
suggest more NO_x that emitted from combustion processes. In contrast, the much higher $\delta^{18}\text{O}$
275 values in Vega et al. (2019) indicate a much greater contribution from O_3 in sub-Arctic
environments. In Fig. 2a, N isotopic differences for NO_x sources are greater ($35\text{\textperthousand}$), than for $\delta^{18}\text{O}$ -
 NO_x . In fact, the oxygen isotope signature of NO_x is mainly chemistry-driven rather than
determined by the source (see discussion below), and thus, $\delta^{18}\text{O}$ measurements cannot be used to
address the uncertainty of the NO_x sources that may remain when just looking at $\delta^{15}\text{N}$ values alone.
280 As shown in Fig. 2b, the $\delta^{15}\text{N}$ values of aerosol NH_4^+ are systematically higher than that of NH_3 .
Significant ε_N during the conversion of gas to aerosol (up to $33\text{\textperthousand}$) has been proposed to alter the
 $\delta^{15}\text{N}$ values during the transformation of the source (NH_3) to the sink (particulate NH_4^+). Indeed,
our compilation of previous results (Fig. 2b) reveals that particulate NH_4^+ (particularly in the
coarse aerosol fraction) is more enriched in ^{15}N than NH_3 (by $> 23\text{\textperthousand}$ on average), as well as NH_4^+
285 in precipitation (by $18\text{\textperthousand}$ on average). This can most likely be attributed to the preferential
absorption $^{14}\text{N}-\text{NH}_3$ associated with washout processes during precipitation (Zheng et al., 2018).
We are aware of the fact that our sample/data set used here is limited, resulting in a relatively large
uncertainty with regards to the N isotope-based source apportionment. However, all $\delta^{15}\text{N}-\text{NH}_4^+$
values in cloudwater samples fall within the observed range of $\delta^{15}\text{N}-\text{NH}_4^+$ values for fine particles
290 ($\text{PM}_{2.5}$), providing putative evidence that NH_4^+ in cloudwater is primarily derived from particulate
 NH_4^+ rather than NH_3 absorption.

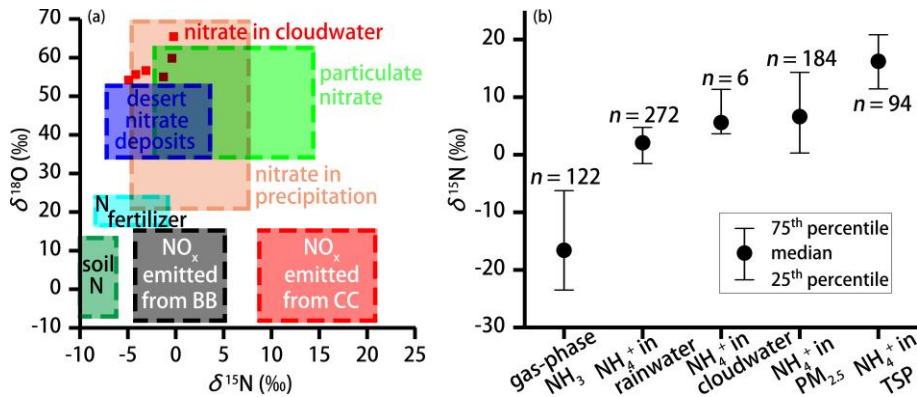


Figure 2. (a) Observed range of typical $\delta^{18}\text{O}$ and $\delta^{15}\text{N}$ values of NO_3^- and NO_x for different sources (adapted from Fenech et al. (2012)). BB and CC represent biomass burning and coal combustion, respectively. The red squares represent nitrate isotope data in cloudwater (this study). (b) The 25th percentiles, median and 75th percentiles for the $\delta^{15}\text{N}$ values of the ambient NH_3 (Chang et al., 2016; Felix et al., 2013; Savard et al., 2018; Smirnoff et al., 2012) and NH_4^+ in precipitation (Fang et al., 2011; Leng et al., 2018; Yang et al., 2014; Zhang et al., 2008), cloudwater (this study), $\text{PM}_{2.5}$ (particulate matter with aerodynamic diameter less than 2.5 μm ; (Lin et al., 2016; Park et al., 2018; Proemse et al., 2012; Smirnoff et al., 2012), and TSP (particulate matter with aerodynamic diameter less than 100 μm (Kundu et al., 2010; Savard et al., 2018; Yeatman et al., 2001) are shown.

3.3 Isotope-based assessment of the sources and formation of nitrogenous species in clouds

Using the MixSIR model, the relative contribution of four NH_3 sources to NH_4^+ can be calculated, based on the isotope data of ambient $\delta^{15}\text{N-NH}_4^+$, and considering the N fractionation and prior information on the site. As upper limit for the N isotope enrichment factor associated with the conversion of NH_3 to NH_4^+ ($\epsilon_{\text{NH}_4^+-\text{NH}_3}$), we assumed 33‰ when using MixSIR, but also considered lower values for $\epsilon_{\text{NH}_4^+-\text{NH}_3}$ (Fig. 3a) (given the conflicting evidence with regards to

$\varepsilon_{\text{NH}_4^+ - \text{NH}_3}$; e.g., Deng et al., 2018; Li et al., 2012). Dependent of the choice for $\varepsilon_{\text{NH}_4^+ - \text{NH}_3}$ (between

310 0‰ to 33‰ proposed by Heaton et al. (1997)) the relative contribution of biomass burning, fertilizer application, and livestock breeding to NH_4^+ in cloudwater ranges from 25.9% to 85.4%,

5.9% to 37.0%, and 8.7% to 85.4%, respectively. Irrespective of the uncertainty related to $\varepsilon_{\text{NH}_4^+ - \text{NH}_3}$,

the measurement of levoglucosan provides compelling evidence that biomass burning represents an important NH_3 source, independently validating our isotope approach. Our sampling site was

315 located in the North China Plain, also known as the granary of China. Although non-agricultural

NH_3 emissions like on-road traffic are important in the urban atmosphere (Chang et al., 2016),

their contribution must be considered insignificant with respect to fertilizer application and

livestock breeding in this region (Kang et al., 2016). Besides, coal-based heating in China is

suspended during summertime, and coal combustion has been demonstrated to be a minor

320 contributor of total NH_3 emissions (Li et al., 2016a). Hence the partitioning between the three main

NH_3 sources appears plausible. Moreover, existing emission inventory data confirm that the ratio

of NH_3 emissions in North China Plain from livestock breeding (1658 kt) and fertilizer application

(1413 kt) was 1.17 (Zhang et al., 2010), which is very close to our estimate (between 0.98 and

1.14) when $\varepsilon_{\text{NH}_4^+ - \text{NH}_3} \geq 25\%$. For a $\varepsilon_{\text{NH}_4^+ - \text{NH}_3}$ range that we consider most plausible (i.e. between

325 25‰ and 33‰), the relative cloudwater NH_4^+ source partitioning between biomass burning,

fertilizer application, and livestock is $32.9 \pm 4.6\%$, $32.9 \pm 3.0\%$, and $34.2 \pm 1.6\%$, respectively

(indicated as red square in Fig. 3a). It is important to note that there was large uncertainty in the

evaluation of biomass burning, which was partly ascribed to the lack of localized isotopic source

signatures in China. In addition, the isotopic fractionation from the conversion of NH_3 to NH_4^+

330 was simplified in this study, and it was not possible to incorporate all of the possible equilibrium

and kinetic fractionation scenarios.

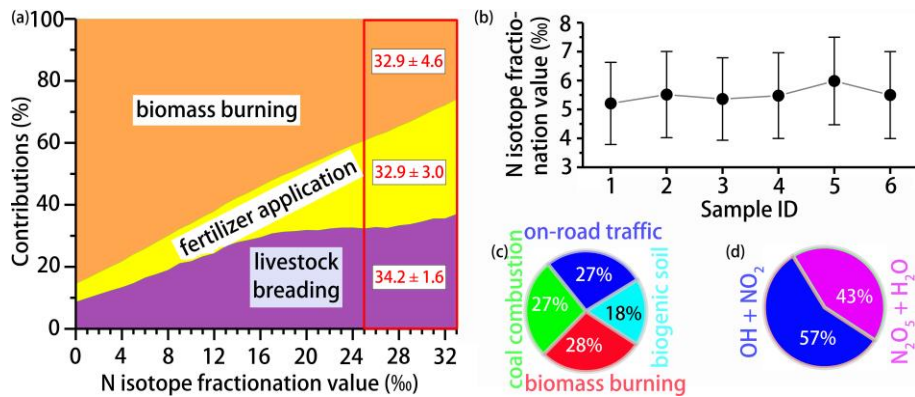


Figure 3. (a) Source partitioning estimates for NH_4^+ in cloudwater as a function of

$\varepsilon_{\text{NH}_3 \rightarrow \text{NH}_4^+}$. The red square highlights the best-guess estimates based on $\varepsilon_{\text{NH}_4^+ - \text{NH}_3} \geq 25\text{\textperthousand}$. (b)

335 Whisker plot of the N fractionation for the conversion of NO_x to NO_3^- ($\varepsilon_{\text{NO}_3^- - \text{NO}_x}$) calculated by the computational quantum chemistry (CQC) module. The upper line, dot, and bottom line indicate the 25th percentile, median, and 75th percentile, respectively. Refer to Table 1 for sample ID. (c) Overall contribution of various NO_x sources to NO_3^- in cloudwater as estimated by the MixSIR model. (d) Overall contribution of the two dominant pathways to NO_3^- formation in cloudwater, 340 as estimated by the MixSIR model.

The computational quantum chemistry (CQC) module in MixSIR has been proven a robust tool to quantify the N isotope enrichment factor during NO_x - NO_3^- conversion ($\varepsilon_{\text{NO}_3^- - \text{NO}_x}$) (e.g., Zong et al., 2017, Chang et al., 2018). Cloudwater sample-based data from this study reveal that $\varepsilon_{\text{NO}_3^- - \text{NO}_x}$ values fall into a small range (5.21‰ to 5.98‰) (Fig. 3b), suggesting robust isotope effects during the N isotopic exchange reactions. Knowing $\varepsilon_{\text{NO}_3^- - \text{NO}_x}$, the overall contribution of various NO_x sources to NO_3^- in cloudwater can be estimated (Fig. 3c). As was expected, biomass burning was the largest contributor ($28.2 \pm 2.7\%$), followed by on-road traffic ($27.1 \pm 2.2\%$), coal combustion ($26.8 \pm 3.4\%$), and biogenic soil ($17.9 \pm 3.9\%$). The fundamental importance of

biomass burning-emitted NO_x to NO_3^- in cloudwater is supported by the observed correlation
350 between the concentrations of levoglucosan and biomass burning-derived NO_3^- ($r^2 = 0.66$). The average contribution ratio of coal combustion and on-road transportation to NO_x emissions in our study (0.99) is slightly lower than that calculated from regional emission inventories (9.0 Tg/7.4 Tg = 1.22) (Zhao et al., 2013). The apparent difference is likely real, and reflects the fact that NO_x emissions by anthropogenic activities changed significantly since 2010: a 17% total emission
355 decrease between 2010 and 2017 can primarily be attributed to upgraded emission standards and new “ultra-low emission” techniques in the coal-fired power plant sector, given that traffic-emitted NO_x likely increased as a consequence of the continuous expansion of auto trade market during the last decade (Chang et al., 2018). In turn, our source partitioning estimate probably reflects the most updated status of NO_x emissions in China, where transportation-related NO_x emissions have
360 reached levels that are comparable to NO_x emissions by coal combustion. In this regard, our study demonstrates that Bayesian-based isotopic mixing modeling can be an effective and timely approach to track rapid emissions changes of NO_x in a fast-developing country like China.

Using the measured $\delta^{18}\text{O}$ and equations 1-4 (and the assumptions above), we can calculate γ , and the relative importance of the two oxidation pathways of NO_3^- formation (Fig. 3d). On
365 average, 57% NO_3^- formation can be attributed to the “ $\text{NO}_2 + \text{OH}$ ” pathway, and 43% to the “ $\text{N}_2\text{O}_5 + \text{H}_2\text{O}$ ” pathway. In the low-latitude regions, where atmospheric OH concentrations are highest, particulate NO_3^- production via the “ $\text{NO}_2 + \text{OH}$ ” pathway predominates (up to 87%) (Alexander et al., 2009). Sampling during summertime, oxidation of NO_2 through OH was expected to be the dominant pathway of nitrate formation, in accordance with observations from the subtropics
370 (Hastings et al., 2003). However, our results highlight that N_2O_5 hydrolysis can be an almost

equally important process as the oxidization of NO_2 with OH with regards to the NO_3^- formation in cloudwater (Wang et al., 2017b).

4 Conclusions

In this study, we measured the isotopic composition of nitrogenous species in cloudwater 375 at the summit of Mt. Tai during a long-lasting biomass burning event, in order to investigate the sources and processes involved in cloudwater $\text{NO}_3^-/\text{NH}_4^+$ formation, and in turn to test our isotope-balance approach to constrain N source partitioning in cloudwater. Using a Bayesian isotope mixing model, the $\delta^{15}\text{N}$ -based estimates confirm that at least transiently biomass burning related NH_3 and NO_x emissions is a major source of cloudwater N. Moreover, our data are in accordance 380 with regional emission inventories for both NH_3 and NO_x , validating the Bayesian isotope mixing model approach. Based on cloud water nitrate $\delta^{18}\text{O}$ measurements, the reaction of NO_2 with OH turned out to be the dominant pathway to form cloud nitrate, yet the contribution from the heterogeneous hydrolysis of N_2O_5 to NO_3^- is almost equally important. Our study underscores the value of cloud-water dissolved inorganic nitrogen isotopes as carrier of quantitative information 385 on regional NO_x emissions. It sheds light on the origin and production pathways of nitrogenous species in clouds and emphasizes the importance of BB-derived nitrogenous species as cloud condensation nuclei in China's troposphere. Moreover, it highlights the rapid evolution of NO_x emissions in China. Despite an overall reduction in total anthropogenic NO_x emission due to effective emission control actions and stricter emission standards for vehicles, the relative 390 contribution of transportation to total NO_x emissions has increased over the last decade and may already have exceeded emissions from the power sector.

Data availability

All data used to support the conclusion are presented in this paper. Additional data are available upon request. Please contact the corresponding authors (Yanlin Zhang
395 (dryanlinzhang@outlook.com) and Jianmin Chen (jmchen@fudan.edu.cn)).

Acknowledgments

This study was supported by the National Key R&D Program of China (Grant no. 2017YFC0212700, task 1 and 4), National Natural Science Foundation of China (Grant nos. 41705100, 91644103), the Provincial Natural Science Foundation of Jiangsu (Grant nos. 400 BK20180040, BK20170946), University Science Research Project of Jiangsu Province (17KJB170011), the University of Basel research funds, the Priority Academic Program Development of Jiangsu Higher Education Institutions (PAPD), and through Program for Changjiang Scholars and Innovative Research Team in University of Ministry of Education of China (PCSIRT).

405 References

Alexander, B., Hastings, M. G., Allman, D. J., Dachs, J., Thornton, J. A., and Kunasek, S. A.: Quantifying atmospheric nitrate formation pathways based on a global model of the oxygen isotopic composition ($\Delta^{17}\text{O}$) of atmospheric nitrate, *Atmos. Chem. Phys.*, 9, 5043-5056, <https://doi.org/10.5194/acp-9-5043-2009>, 2009.

410 Anenberg, S. C., Miller, J., Minjares, R., Du, L., Henze, D. K., Lacey, F., Malley, C. S., Emberson, L., Franco, V., Klimont, Z., Heyes, C.: Impacts and mitigation of excess diesel-related NO_x emissions in 11 major vehicle markets. *Nature*, 545, 467-471, 2017.

Balasubramanian, S., Koloutsou-Vakakis, S., McFarland, D. M., Rood, M. J.: Reconsidering emissions of ammonia from chemical fertilizer usage in Midwest USA, *J. Geophys. Res.*, 415 120, 6232-6246, 2015.

Benkovitz, C. M., Scholtz M. T., Pacyna J., Tarrasón L., Dignon J., Voldner E. C., Spiro P. A., Logan J. A., and Graedel T. E.: Global gridded inventories of anthropogenic emissions of sulfur and nitrogen, *J. Geophys. Res.*, 101, 29239-29253, <https://doi.org/10.1029/96JD00126>, 1996.

420 Boone, E. J., Laskin, A., Laskin, J., Wirth, C., Shepson, P. B., Stirm, B. H., and Pratt, K. A.: Aqueous processing of atmospheric organic particles in cloud water collected via aircraft sampling, *Environ. Sci. Technol.*, 49, 8523-8530, <https://doi.org/10.1021/acs.est.5b01639>, 2015.

425 Bouwman, A., Lee, D., Asman, W., Dentener, F., Van Der Hoek, K., and Olivier, J.: A global high-resolution emission inventory for ammonia, *Global Biogeochem. Cy.*, 11, 561-587, <https://doi.org/10.1029/97GB02266>, 1997.

430 Cao, F., Zhang, S. C., Kawamura, K., and Zhang, Y. L.: Inorganic markers, carbonaceous components and stable carbon isotope from biomass burning aerosols in Northeast China, *Sci. Total Environ.*, 572, 1244-1251, <https://doi.org/10.1016/j.scitotenv.2015.09.099>, 2016, 2016.

435 Cao, F., Zhang, S. C., Kawamura, K., Liu, X., Yang, C., Xu, Z., Fan, M., Zhang, W., Bao, M., Chang, Y., Song, W., Liu, S., Lee, X., Li, J., Zhang, G., and Zhang, Y. L.: Chemical characteristics of dicarboxylic acids and related organic compounds in PM_{2.5} during biomass-burning and non-biomass-burning seasons at a rural site of Northeast China, *Environ. Pollut.*, 231, 654-662, <https://doi.org/10.1016/j.envpol.2017.08.045>, 2017.

440 Chang, Y. H., Liu, X., Deng, C., Dore, A. J., and Zhuang, G.: Source apportionment of atmospheric ammonia before, during, and after the 2014 APEC summit in Beijing using stable nitrogen isotope signatures, *Atmos. Chem. Phys.*, 16, 11635-11647, <https://doi.org/10.5194/acp-16-11635-2016>, 2016.

445 Chang, Y. H., Zhang, Y., Tian, C., Zhang, S., Ma, X., Cao, F., Liu, X., Zhang, W., Kuhn, T., and Lehmann, M. F.: Nitrogen isotope fractionation during gas-to-particle conversion of NO_x to NO₃⁻ in the atmosphere - implications for isotope-based NO_x source apportionment, *Atmos. Chem. Phys.*, 18, 11647-11661, <https://doi.org/10.5194/acp-18-11647-2018>, 2018.

450 Chellman, N. J., Hastings, M. G., and McConnell, J. R.: Increased nitrate and decreased δ¹⁵N-NO₃⁻ in the Greenland Arctic after 1940 attributed to North American oil burning, *Cryosphere Discus*, <https://doi.org/10.5194/tc-2016-163>, 2016.

455 Chen, J. M., Li, C., Ristovski, Z., Milic, A., Gu, Y., Islam, M. S., Wang, S., Hao, J., Zhang, H., He, C., Guo, H., Fu, H., Miljevic, B., Morawska, L., Thai, P., Lam, Y. F., Pereira, G., Ding, A., Huang, X., and Dumka, U. C.: A review of biomass burning: Emissions and impacts on air quality, health and climate in China, *Sci. Total Environ.*, 579, 1000-1034, <https://doi.org/10.1016/j.scitotenv.2016.11.025>, 2017.

Chen, Y. C., Christensen, M. W., Stephens, G. L., and Seinfeld, J. H.: Satellite-based estimate of global aerosol-cloud radiative forcing by marine warm clouds, *Nature Geosci.*, 7, 643, <https://doi.org/10.1038/ngeo2214>, 2014.

455 Crutzen, P. J., and Andreae, M. O.: Biomass burning in the tropics: Impact on atmospheric chemistry and biogeochemical cycles. *Science*, 250(4988), 1669-1678, <https://doi.org/10.1126/science.250.4988.1669>, 1990.

Demoz, B. B., Collett, J. L., and Daube, B. C.: On the Caltech active strand cloudwater collectors, *Atmos. Res.*, 41, 47-62, [https://doi.org/10.1016/0169-8095\(95\)00044-5](https://doi.org/10.1016/0169-8095(95)00044-5), 1996.

460 Deng, Y., Li, Y., and Li, L.: Experimental investigation of nitrogen isotopic effects associated with ammonia degassing at 0-70 °C, *Geochim. Cosmochim. Ac.*, 226, 182-191, <https://doi.org/10.1016/j.gca.2018.02.007>, 2018.

465 Desyaterik, Y., Sun, Y., Shen, X., Lee, T., Wang, X., Wang, T., and Collett, J. L.: Speciation of “brown” carbon in cloud water impacted by agricultural biomass burning in eastern China, *J. Geophys. Res.*, 118, 7389-7399, <https://doi.org/10.1002/jgrd.50561>, 2013.

470 Duncan, B. N., Lamsal, L. N., Thompson, A. M., Yoshida, Y., Lu, Z., Streets, D. G., Hurwitz, M. M., Pickering, K. E.: A space-based, high-resolution view of notable changes in urban NO_x pollution around the world (2005-2014), *J. Geophys. Res.*, 121, 976-996, 2016.

475 Elliott, E., Kendall, C., Wankel, S. D., Burns, D., Boyer, E., Harlin, K., Bain, D., and Butler, T.: Nitrogen isotopes as indicators of NO_x source contributions to atmospheric nitrate deposition across the Midwestern and northeastern United States, *Environ. Sci. Technol.*, 41, 7661-7667, <https://doi.org/10.1021/es070898t>, 2007.

480 Elliott, E. M., Kendall, C., Boyer, E. W., Burns, D. A., Lear, G. G., Golden, H. E., Harlin, K., Bytnarowicz, A., Butler, T. J., and Glatz, R.: Dual nitrate isotopes in dry deposition: Utility for partitioning NO_x source contributions to landscape nitrogen deposition, *J. Geophys. Res.*, 114, <https://doi.org/10.1029/2008jg000889>, 2009.

485 Fang, Y. T., Koba, K., Wang, X. M., Wen, D. Z., Li, J., Takebayashi, Y., Liu, X. Y., and Yoh, M.: Anthropogenic imprints on nitrogen and oxygen isotopic composition of precipitation nitrate in a nitrogen-polluted city in southern China, *Atmos. Chem. Phys.*, 11, 1313-1325, <https://doi.org/10.5194/acp-11-1313-2011>, 2011.

490 Felix J. D., and E. M. Elliott.: The agricultural history of human-nitrogen interactions as recorded in ice core $\delta^{15}\text{N-NO}_3^-$, *Geophys. Res. Lett.*, 40, 1642-1646, <https://doi.org/10.1002/grl.50209>, 2013.

495 Felix, J. D., and Elliott, E. M.: Isotopic composition of passively collected nitrogen dioxide emissions: Vehicle, soil and livestock source signatures, *Atmos. Environ.*, 92, 359-366, <https://doi.org/10.1016/j.atmosenv.2014.04.005>, 2014.

500 Felix, J. D., Elliott, E. M., Avery, G. B., Kieber, R. J., Mead, R. N., Willey, J. D., and Mullaugh, K. M.: Isotopic composition of nitrate in sequential Hurricane Irene precipitation samples: Implications for changing NO_x sources, *Atmos. Environ.*, 106, 191-195, <https://doi.org/10.1016/j.atmosenv.2015.01.075>, 2015.

Felix, J. D., Elliott, E. M., Gish, T. J., McConnell, L. L., and Shaw, S. L.: Characterizing the isotopic composition of atmospheric ammonia emission sources using passive samplers and a combined oxidation-bacterial denitrifier approach, *Rapid Commun. Mass Sp.*, 27, 2239-2246, <https://doi.org/10.1002/rcm.6679>, 2013.

Felix, J. D., Elliott, E. M., and Shaw, S. L.: Nitrogen isotopic composition of coal-fired power plant NO_x: Influence of emission controls and implications for global emission inventories, *Environ. Sci. Technol.*, 46, 3528-3535, <https://doi.org/10.1021/es203355v>, 2012.

Fenech, C., Rock, L., Nolan, K., Tobin, J., and Morrissey, A.: The potential for a suite of isotope and chemical markers to differentiate sources of nitrate contamination: a review. *Water Res.*, 46, 2023-2041, <https://doi.org/10.1016/j.watres.2012.01.044>, 2012.

Fibiger, D. L., and Hastings, M. G.: First measurements of the nitrogen isotopic composition of NO_x from biomass burning, *Environ. Sci. Technol.*, 50, 11569-11574. 10.1021/acs.est.6b03510, 2016.

Fomba, K. W., van Pinxteren, D., Müller, K., Iinuma, Y., Lee, T., Collett, J. L., and Herrmann, H.: 505 Trace metal characterization of aerosol particles and cloud water during HCCT 2010, *Atmos. Chem. Phys.*, 15, 8751-8765, <https://doi.org/10.5194/acp-15-8751-2015>, 2015.

Gioda, A., Reyes-Rodríguez, G. J., Santos-Figueroa, G., Collett, J. L., Decesari, S., Ramos, M. d. C. K. V., Bezerra Netto, H. J. C., de Aquino Neto, F. R., and Mayol-Bracero, O. L.: Speciation of water-soluble inorganic, organic, and total nitrogen in a background marine 510 environment: Cloud water, rainwater, and aerosol particles, *J. Geophys. Res.*, 116, <https://doi.org/10.1029/2010JD015010>, 2011.

Hastings, M., Casciotti, K. L., and Elliott, E. M.: Stable isotopes as tracers of anthropogenic nitrogen sources, deposition, and impacts. *Elements*, 9, 339-344, <https://doi.org/10.2113/gselements.9.5.339>, 2013.

Hastings, M., Jarvis, J., and Steig, E.: Anthropogenic impacts on nitrogen isotopes of ice-core 515 nitrate. *Science*, 324, 1288, <https://doi.org/10.1126/science.1170510>, 2009.

Hastings, M., Sigman, D. M., and Lipschultz, F.: Isotopic evidence for source changes of nitrate in rain at Bermuda, *J. Geophys. Res.*, 108, <https://doi.org/10.1029/2003JD003789>, 2003.

Heald, C. L., Collett Jr, J., Lee, T., Benedict, K., Schwandner, F., Li, Y., Clarisse, L., Hurtmans, 520 D., Van Damme, M., Clerbaux, C.: Atmospheric ammonia and particulate inorganic nitrogen over the United States, *Atmos. Chem. Phys.*, 12(21), 10295-10312, 2012.

Heaton, T. H. E., Spiro, B., and Robertson, S. M. C.: Potential canopy influences on the isotopic composition of nitrogen and sulphur in atmospheric deposition. *Oecologia*, 109, 600-607, <https://doi.org/10.1007/s004420050122>, 1997.

Herrmann, H., Schaefer, T., Tilgner, A., Styler, S. A., Weller, C., Teich, M., and Otto, T.: 525 Tropospheric aqueous-phase chemistry: Kinetics, mechanisms, and its coupling to a changing gas phase. *Chem. Reviews*, 115, 4259-4334, <https://doi.org/10.1021/cr500447k>, 2015.

Hoffmann, D., Tilgner, A., Iinuma, Y., and Herrmann, H.: Atmospheric stability of levoglucosan: 530 A detailed laboratory and modeling study, *Environ. Sci. Technol.*, 44, 694-699, <https://doi.org/10.1021/es902476f>, 2010.

Huang, C., Chen, C. H., Li, L., Cheng, Z., Wang, H. L., Huang, H. Y., Streets, D. G., Wang, Y. J., Zhang, G. F., Chen, Y. R.: Emission inventory of anthropogenic air pollutants and VOC species in the Yangtze River Delta region, China, *Atmos. Chem. Phys.*, 11, 4105-4120, 535 2011.

Jaegle, L., Steinberger, L., Martin, R. V., Chance, K.: Global partitioning of NO_x sources using satellite observations: Relative roles of fossil fuel combustion, biomass burning and soil emissions. *Faraday Discuss.*, 130, 407-423, 2005.

Kang, Y., Liu, M., Song, Y., Huang, X., Yao, H., Cai, X., Zhang, H., Kang, L., Liu, X., Yan, X., He, H., Zhang, Q., Shao, M., and Zhu, T.: High-resolution ammonia emissions inventories 540

in China from 1980 to 2012, *Atmos. Chem. Phys.*, 16, 2043-2058, <https://doi.org/10.5194/acp-16-2043-2016>, 2016.

Kawashima, H., and Kurahashi, T.: Inorganic ion and nitrogen isotopic compositions of atmospheric aerosols at Yurihonjo, Japan: Implications for nitrogen sources, *Atmos. Environ.*, 45, 6309-6316, <https://doi.org/10.1016/j.atmosenv.2011.08.057>, 2011.

Kim, I. N., Lee, K., Gruber, N., Karl, D. M., Bullister, J. L., Yang, S., and Kim, T. W.: Increasing anthropogenic nitrogen in the North Pacific Ocean. *Science*, 346, 1102-1106, <https://doi.org/10.1126/science.1258396>, 2014.

Kundu, S., Kawamura, K., and Lee, M.: Seasonal variation of the concentrations of nitrogenous species and their nitrogen isotopic ratios in aerosols at Gosan, Jeju Island: Implications for atmospheric processing and source changes of aerosols, *J. Geophys. Res.*, 115, <https://doi.org/10.1029/2009JD013323>, 2010.

Lamsal, L. N., Martin, R. V., Padmanabhan, A., van Donkelaar, A., Zhang, Q., Sioris, C. E., Chance, K., Kurosu, T. P., Newchurch, M. J.: Application of satellite observations for timely updates to global anthropogenic NO_x emission inventories, *Geophys. Res. Lett.*, 38, (5), <https://doi.org/10.1029/2010GL046476>, 2011.

Lance, S., Barth, M., and Carlton, A.: Multiphase chemistry: Experimental design for coordinated measurement and modeling studies of cloud processing at a mountaintop, *B. Am. Meteorol. Soc.*, 98, ES163-ES167, <https://doi.org/10.1175/bams-d-17-0015.1>, 2017.

Leng, Q., Cui, J., Zhou, F., Du, K., Zhang, L., Fu, C., Liu, Y., Wang, H., Shi, G., Gao, M., Yang, F., and He, D.: Wet-only deposition of atmospheric inorganic nitrogen and associated isotopic characteristics in a typical mountain area, southwestern China, *Sci. Total Environ.*, 616, 55-63, <https://doi.org/10.1016/j.scitotenv.2017.10.240>, 2017.

Levy, H., Moxim, W. J., Kasibhatla, P. S.: A global three-dimensional time-dependent lightning source of tropospheric NO_x, *J. Geophys. Res.*, 101, 22911-22922, 1996.

Li, J., Wang, X., Chen, J., Zhu, C., Li, W., Li, C., Liu, L., Xu, C., Wen, L., Xue, L., Wang, W., Ding, A., and Herrmann, H.: Chemical composition and droplet size distribution of cloud at the summit of Mount Tai, China, *Atmos. Chem. Phys.*, 17, 9885-9896, <https://doi.org/10.5194/acp-17-9885-2017>, 2017.

Li, L., Lollar, B. S., Li, H., Wortmann, U. G., and Lacrampe-Couloume, G.: Ammonium stability and nitrogen isotope fractionations for NH₃(aq)-NH₃(gas) systems at 20-70 °C and pH of 2-13: Applications to habitability and nitrogen cycling in low-temperature hydrothermal systems, *Geochim. Cosmochim. Ac.*, 84, 280-296, <https://doi.org/10.1016/j.gca.2012.01.040>, 2012.

Li, Q., Jiang, J., Cai, S., Zhou, W., Wang, S., Duan, L., and Hao, J.: Gaseous ammonia emissions from coal and biomass combustion in household stoves with different combustion efficiencies, *Environ. Sci. Technol. Lett.*, 3, 98-103, <https://doi.org/10.1021/acs.estlett.6b00013>, 2016a.

Li, T., Wang, Y., Mao, H., Wang, S., Talbot, R. W., Zhou, Y., Wang, Z., Nie, X., and Qie, G.: Insights on chemistry of mercury species in clouds over Northern China: Complexation and adsorption, *Environ. Sci. Technol.*, 52, 5125-5134, <https://doi.org/10.1021/acs.est.7b06669>, 2018.

585 Li, Y., Schichtel, B. A., Walker, J. T., Schwede, D. B., Chen, X., Lehmann, C. M. B., Puchalski, M. A., Gay, D. A., and Collett, J. L.: Increasing importance of deposition of reduced nitrogen in the United States, *P. Natl. Acad. Sci. USA.*, <https://doi.org/10.1073/pnas.1525736113>, 2016b.

590 Lin, C. T., Jickells, T. D., Baker, A. R., Marca, A., and Johnson, M. T.: Aerosol isotopic ammonium signatures over the remote Atlantic Ocean, *Atmos. Environ.*, 133, 165-169, <https://doi.org/10.1016/j.atmosenv.2016.03.020>, 2016.

595 Lin, Q., Zhang, G., Peng, L., Bi, X., Wang, X., Brechtel, F. J., Li, M., Chen, D., Peng, P., Sheng, G., and Zhou, Z.: In situ chemical composition measurement of individual cloud residue particles at a mountain site, southern China, *Atmos. Chem. Phys.*, 17, 8473-8488, <https://doi.org/10.5194/acp-17-8473-2017>, 2017.

Liu, D., Fang, Y., Tu, Y., and Pan, Y.: Chemical method for nitrogen isotopic analysis of ammonium at natural abundance, *Anal. Chem.*, 86, 3787-3792, <https://doi.org/10.1021/ac403756u>, 2014.

600 Liu, X., Zhang, Y., Han, W., Tang, A., Shen, J., Cui, Z., Vitousek, P., Erisman, J. W., Goulding, K., Christie, P., Fangmeier, A., and Zhang, F.: Enhanced nitrogen deposition over China. *Nature*, 494, 459-462, <https://doi.org/10.1038/nature11917>, 2013.

605 Liu, L., Zhang, J., Xu, L., Yuan, Q., Huang, D., Chen, J., Shi, Z., Sun, Y., Fu, P., Wang, Z., Zhang, D., and Li, W.: Cloud scavenging of anthropogenic refractory particles at a mountain site in North China, *Atmos. Chem. Phys.*, 18, 14681-14693, <https://doi.org/10.5194/acp-18-14681-2018>, 2018.

Lobert, J. M., Scharffe, D. H., Hao, W. M., and Crutzen, P. J.: Importance of biomass burning in the atmospheric budgets of nitrogen-containing gases. *Nature*, 346, 552, <https://doi.org/10.1038/346552a0>, 1990.

610 McIlvin, M. R., and Altabet, M. A.: Chemical conversion of nitrate and nitrite to nitrous oxide for nitrogen and oxygen isotopic analysis in freshwater and seawater, *Anal. Chem.*, 77, 5589-5595, <https://doi.org/10.1021/ac050528s>, 2005.

615 Michalski, G., Bockheim, J. G., Kendall, C., and Thiemens, M.: Isotopic composition of Antarctic Dry Valley nitrate: Implications for NO_y sources and cycling in Antarctica, *Geophys. Res. Lett.*, 32, <https://doi.org/10.1029/2004GL022121>, 2005.

Michalski, G., Bhattacharya, S., and Mase, F.: Oxygen isotope dynamics of atmospheric nitrate and its precursor molecules (Chapter 30), in M. Baskaran (ed.), *Handbook of Environmental Isotope Geochemistry, Advances in Isotope Geochemistry*, https://doi.org/10.1007/978-3-642-10637-8_30, Springer-Verlag, Berlin Heidelberg, 2011.

Miyazaki, K., Eskes, H., Sudo, K., Boersma, K. F., Bowman, K., Kanaya, Y.: Decadal changes in global surface NO_x emissions from multi-constituent satellite data assimilation, *Atmos. Chem. Phys.*, 17, 807-837, 2017.

620 Morin, S., Savarino, J., Frey, M. M., Yan, N., Bekki, S., Bottenheim, J. W., and Martins, J. M.: Tracing the origin and fate of NO_x in the Arctic atmosphere using stable isotopes in nitrate. *Science*, 322, 730-732, <https://doi.org/10.1126/science.1161910>, 2008.

625 Morino, Y., Kondo, Y., Takegawa, N., Miyazaki, Y., Kita, K., Komazaki, Y., Fukuda, M., Miyakawa, T., Moteki, N., Worsnop, D. R.: Partitioning of HNO_3 and particulate nitrate over Tokyo: Effect of vertical mixing, *J. Geophys. Res.*, 111, <https://doi.org/10.1029/2005JD006887>, 2006.

630 Norris, J. R., Allen, R. J., Evan, A. T., Zelinka, M. D., O'Dell, C. W., and Klein, S. A.: Evidence for climate change in the satellite cloud record. *Nature*, 536, 72, <https://doi.org/10.1038/nature18273>, 2016.

635 Okin, G. S., Baker, A. R., Tegen, I., Mahowald, N. M., Dentener, F. J., Duce, R. A., Galloway, J. N., Hunter, K., Kanakidou, M., Kubilay, N., Prospero, J. M., Sarin, M., Surapipith, V., Uematsu, M., and Zhu, T.: Impacts of atmospheric nutrient deposition on marine productivity: Roles of nitrogen, phosphorus, and iron. *Global Biogeochem. Cy.*, 25, <https://doi.org/10.1029/2010GB003858>, 2011.

640 Olivier, J., Bouwman, A., Van der Hoek, K., and Berdowski, J.: Global air emission inventories for anthropogenic sources of NO_x , NH_3 and N_2O in 1990, *Environ. Pollut.*, 102, 135-148, <https://doi.org/10.1016/B978-0-08-043201-4.50024-1>, 1998.

645 Park, Y., Park, K., Kim, H., Yu, S., Noh, S., Kim, M., Kim, J., Ahn, J., Lee, M., Seok, K., and Kim, Y.: Characterizing isotopic compositions of TC-C, NO_3^- -N, and NH_4^+ -N in $\text{PM}_{2.5}$ in South Korea: Impact of China's winter heating, *Environ. Pollut.*, 233, 735-744, <https://doi.org/10.1016/j.envpol.2017.10.072>, 2018.

650 Paulot, F. and Jacob, D. J.: Hidden cost of US agricultural exports: particulate matter from ammonia emissions, *Environ. Sci. Technol.*, 48, 903-908, 2014.

655 Proemse, B. C., Mayer, B., Chow, J. C., and Watson, J. G.: Isotopic characterization of nitrate, ammonium and sulfate in stack $\text{PM}_{2.5}$ emissions in the Athabasca Oil Sands Region, Alberta, Canada, *Atmos. Environ.*, 60, 555-563, <https://doi.org/10.1016/j.atmosenv.2012.06.046>, 2012.

Price, C., Penner, J., Prather, M.: NO_x from lightning: 1. Global distribution based on lightning physics, *J. Geophys. Res.*, 102, 5929-5941, 1997.

660 Ravishankara, A. R.: Heterogeneous and multiphase chemistry in the troposphere. *Science*, 276, 1058-1065, <https://doi.org/10.1126/science.276.5315.1058>, 1997.

Reche, C., Viana, M., Pandolfi, M., Alastuey, A., Moreno, T., Amato, F., Ripoll, A., Querol, X.: Urban NH_3 levels and sources in a Mediterranean environment, *Atmos. Environ.*, 57, 153-164, 2012.

Reis, S., Pinder, R. W., Zhang, M., Lijie, G., Sutton, M. A.: Reactive nitrogen in atmospheric emission inventories, *Atmos. Chem. Phys.*, 9, 7657-7677, 2009.

Richter, A., Burrows, J. P., Nuss, H., Granier, C., Niemeier, U.: Increase in tropospheric nitrogen dioxide over China observed from space. *Nature*, 437, 129-132, 2005.

Sang, X. F., Gensch, I., Kammer, B., Khan, A., Kleist, E., Laumer, W., Schlag, P., Schmitt, S. H., Wildt, J., Zhao, R., Mungall, E. L., Abbatt, J. P. D., and Kiendler-Scharr, A.: Chemical stability of levoglucosan: an isotopic perspective, *Geophys. Res. Lett.*, 43, 5419-5424, <https://doi.org/10.1002/2016GL069179>, 2016.

665 Savard, M. M., Cole, A. S., Vet, R., and Smirnoff, A.: The $\Delta^{17}\text{O}$ and $\delta^{18}\text{O}$ values of atmospheric nitrates simultaneously collected downwind of anthropogenic sources - implications for polluted air masses, *Atmos. Chem. Phys.*, 18, 10373-10389, <https://doi.org/10.5194/acp-18-10373-2018>, 2018.

670 Seinfeld, J. and Pandis, S. N.: *Atmospheric Chemistry and Physics: From air pollution to climate change*. John Wiley and Sons, 2012.

675 Schlesinger, W., and Hartley, A.: A global budget for atmospheric NH_3 . *Biogeochem.*, 15, 191-211, <https://doi.org/10.1007/BF00002936>, 1992.

Schurman, M. I., Boris, A., Desyaterik, Y., and Collett, J. L.: Aqueous secondary organic aerosol formation in ambient cloud water photo-oxidations, *Aerosol Air Qual. Res.*, 18, 15-25, <https://doi.org/10.4209/aaqr.2017.01.0029>, 2018.

680 Seinfeld, J. H., Bretherton, C., Carslaw, K. S., Coe, H., DeMott, P. J., Dunlea, E. J., Feingold, G., Ghan, S., Guenther, A. B., Kahn, R., Kraucunas, I., Kreidenweis, S. M., Molina, M. J., Nenes, A., Penner, J. E., Prather, K. A., Ramanathan, V., Ramaswamy, V., Rasch, P. J., Ravishankara, A. R., Rosenfeld, D., Stephens, G., and Wood, R.: Improving our fundamental understanding of the role of aerosol-cloud interactions in the climate system, *P. Natl. Acad. Sci. USA.*, 113, 5781-5790, <https://doi.org/10.1073/pnas.1514043113>, 2016.

685 Slade, J. H., Shiraiwa, M., Arangio, A., Su, H., Pöschl, U., Wang, J., and Knopf, D. A.: Cloud droplet activation through oxidation of organic aerosol influenced by temperature and particle phase state, *Geophys. Res. Lett.*, 44, 1583-1591, <https://doi.org/10.1002/2016GL072424>, 2017.

690 Smirnoff, A., Savard, M. M., Vet, R., and Simard, M. C.: Nitrogen and triple oxygen isotopes in near-road air samples using chemical conversion and thermal decomposition, *Rapid Commun. Mass Sp.*, 26, 2791-2804, <https://doi.org/10.1002/rcm.6406>, 2012.

Souri, A. H., Choi, Y., Jeon, W., Kochanski, A. K., Diao, L., Mandel, J., Bhave, P. V., and Pan, S.: Quantifying the impact of biomass burning emissions on major inorganic aerosols and their precursors in the U.S., *J. Geophys. Res.*, 122, 12, <https://doi.org/10.1002/2017JD026788>, 2017.

695 Suarez-Bertoa, R., Zardini, A. A., Astorga, C.: Ammonia exhaust emissions from spark ignition vehicles over the New European Driving Cycle, *Atmos. Environ.*, 97, 43-53, 2014.

Teng, X., Hu, Q., Zhang, L., Qi, J., Shi, J., Xie, H., Gao, H., Yao, X.: Identification of major sources of atmospheric NH_3 in an urban environment in Northern China during wintertime, *Environ. Sci. Technol.*, 51, 6839-6848, 2017.

700 Tu, Y., Fang, Y., Liu, D., and Pan, Y.: Modifications to the azide method for nitrate isotope analysis, *Rapid Commun. Mass Sp.*, 30, 1213-1222, <https://doi.org/10.1002/rcm.7551>, 2016.

van Pinxteren, D., Fomba, K. W., Mertes, S., Müller, K., Spindler, G., Schneider, J., Lee, T., Collett, J. L., and Herrmann, H.: Cloud water composition during HCCT-2010: Scavenging efficiencies, solute concentrations, and droplet size dependence of inorganic ions and dissolved organic carbon, *Atmos. Chem. Phys.*, 16, 3185-3205, <https://doi.org/10.5194/acp-16-3185-2016>, 2016.

705 Vega, C., Mårtensson, M., Wideqvist, U., Kaiser, J., Zieger, P., and Ström, J.: Composition, isotopic fingerprint and source attribution of nitrate deposition from rain and fog at a Sub-Arctic Mountain site in Central Sweden (Mt Åreskutan), *Tellus B*, 71, 1445379, <https://doi.org/10.1080/16000889.2018.1559398>, 2019.

710 Voigt, A., and Shaw, T. A.: Circulation response to warming shaped by radiative changes of clouds and water vapour, *Nature Geosci.*, 8, 102-106, <https://doi.org/10.1038/ngeo2345>, 2015.

715 Walters, W. W., Goodwin, S. R., and Michalski, G.: Nitrogen stable isotope composition ($\delta^{15}\text{N}$) of vehicle-emitted NO_x , *Environ. Sci. Technol.*, 49, 2278-2285, <https://doi.org/10.1021/es505580v>, 2015.

720 Walters, W. W., and Michalski, G.: Theoretical calculation of nitrogen isotope equilibrium exchange fractionation factors for various NO_y molecules, *Geochim. Cosmochim. Ac.*, 164, 284-297, <https://doi.org/10.1016/j.gca.2015.05.029>, 2015.

725 Walters, W. W., Simonini, D. S., and Michalski, G.: Nitrogen isotope exchange between NO and NO_2 and its implications for $\delta^{15}\text{N}$ variations in tropospheric NO_x and atmospheric nitrate, *Geophys. Res. Lett.*, 43, 440-448, <https://doi.org/10.1002/2015gl066438>, 2016.

730 Walters, W. W., Tharp, B. D., Fang, H., Kozak, B. J., and Michalski, G.: Nitrogen isotope composition of thermally produced NO_x from various fossil-fuel combustion sources, *Environ. Sci. Technol.*, 49, 11363-11371, <https://doi.org/10.1021/acs.est.5b02769>, 2015.

735 Wang, Y. L., Liu, X. Y., Song, W., Yang, W., Han, B., Dou, X. Y., Zhao, X. D., Song, Z. L., Liu, C. Q., and Bai, Z. P.: Source appointment of nitrogen in $\text{PM}_{2.5}$ based on bulk $\delta^{15}\text{N}$ signatures and a Bayesian isotope mixing model, *Tellus B*, 69, 1299672, <https://doi.org/10.1080/16000889.2017.1299672>, 2017a.

740 Wang, Z., Wang, W., Tham, Y. J., Li, Q., Wang, H., Wen, L., Wang, X., Wang, T.: Fast heterogeneous N_2O_5 uptake and ClNO_2 production in power plant and industrial plumes observed in the nocturnal residual layer over the North China Plain, *Atmos. Chem. Phys.*, 17, 12361-12378, 2017b.

745 Weathers, K. C., and Likens, G. E.: Clouds in Southern Chile: An important source of nitrogen to nitrogen-limited ecosystems?, *Environ. Sci. Technol.*, 31, 210-213, <https://doi.org/10.1021/es9603416>, 1997.

750 Yang, J. Y. T., Hsu, S. C., Dai, M. H., Hsiao, S. S. Y., and Kao, S. J.: Isotopic composition of water-soluble nitrate in bulk atmospheric deposition at Dongsha Island: Sources and implications of external N supply to the northern South China Sea. *Biogeosci.*, 11, 1833-1846, <https://doi.org/10.5194/bg-11-1833-2014>, 2014.

755 Yeatman, S., Spokes, L., Dennis, P., and Jickells, T.: Comparisons of aerosol nitrogen isotopic composition at two polluted coastal sites, *Atmos. Environ.*, 35, 1307-1320, [https://doi.org/10.1016/S1352-2310\(00\)00408-8](https://doi.org/10.1016/S1352-2310(00)00408-8), 2001.

760 Yienger, J. J. and Levy, H.: Empirical model of global soil-biogenic NO_x emissions, *J. Geophys. Res.*, 100, 11447-11464, 1995.

765 Zhang, C., Geng, X., Wang, H., Zhou, L., Wang, B.: Emission factor for atmospheric ammonia from a typical municipal wastewater treatment plant in South China, *Environ. Pollut.*, 220, 963-970, 2017.

745 Zhang, L., Chen, Y., Zhao, Y., Henze, D. K., Zhu, L., Song, Y., Paulot, F., Liu, X., Pan, Y., Lin, Y., Huang, B.: Agricultural ammonia emissions in China: Reconciling bottom-up and top-down estimates, *Atmos. Chem. Phys.*, 18, 339-355, 2018.

750 Zhang, Y. L., and Cao, F.: Is it time to tackle PM_{2.5} air pollution in China from biomass-burning emissions?, *Environ. Pollut.*, 202, 217-219, <https://doi.org/10.1016/j.envpol.2015.02.005>, 2015.

Zhang, Y., Zheng, L. X., Liu, X. J., Jickells, T., Cape, J. N., Goulding, K., Fangmeier, A., and Zhang, F. S.: Evidence for organic N deposition and its anthropogenic sources in China, *Atmos. Environ.*, 42, 1035-1041, <https://doi.org/10.1016/j.atmosenv.2007.12.015>, 2008.

755 Zhang, Y., Dore, A. J., Ma, L., Liu, X. J., Ma, W. Q., Cape, J. N., and Zhang, F. S.: Agricultural ammonia emissions inventory and spatial distribution in the North China Plain, *Environ. Pollut.*, 158, 490-501, <https://doi.org/10.1016/j.atmosenv.2007.12.015>, 2010.

Zhao, Y., Zhang, J., and Nielsen, C. P.: The effects of recent control policies on trends in emissions of anthropogenic atmospheric pollutants and CO₂ in China, *Atmos. Chem. Phys.*, 13, 487-508, <https://doi.org/10.5194/acp-13-487-2013>, 2013.

760 Zheng, X. D., Liu, X. Y., Song, W., Sun, X. C., and Liu, C. Q.: Nitrogen isotope variations of ammonium across rain events: Implications for different scavenging between ammonia and particulate ammonium, *Environ. Pollut.*, 239, 392-398, <https://doi.org/10.1016/j.envpol.2018.04.015>, 2018.

Zong, Z., Wang, X., Tian, C., Chen, Y., Fang, Y., Zhang, F., Li, C., Sun, J., Li, J., and Zhang, G.: 765 First assessment of NO_x sources at a regional background site in North China using isotopic analysis linked with modeling, *Environ. Sci. Technol.*, 51, <https://doi.org/10.1021/acs.est.6b06316>, 2017.